FREQUENCY AND SCALE EFFECTS IN THE OPTIMIZATION OF ACOUSTIC WAVEFORM LOGS

by

Frederick L. Paillet

U. S. Geological Survey
Denver, Colorado

ABSTRACT

Previously formulated scaling laws relating acoustic waveforms in boreholes to frequency, tool size and borehole diameter were investigated by repeated logging of the same test interval with different frequencies, and by logging adjacent boreholes of different diameters with the same logging system. Acoustic source frequency bands were centered on approximately 15, 20 and 34 kilohertz. Borehole diameters were 8 and 17 centimeters for test intervals located at depths ranging from 100 to 400 meters in granite. Test intervals included zones of homogeneous rock and fracture zones that were independently characterized with acoustic televiewer logs and core from the 8 centimeter borehole. The high frequency transducer produced waveforms dominated by the tube wave mode in the 8 centimeter borehole, but by a complicated interference pattern produced by the superposition of three normal modes in the 17 centimeter borehole. The two lower frequency transducers produced waveforms in the 17 centimeter diameter borehole with power spectra dominated by the first normal mode. Various methods for picking shear arrivals produced shear velocities in close agreement with known values for all cases except for the data obtained with the high frequency transducer in the 17 centimeter diameter borehole. This result was attributed to the effects of mode superposition and enhanced attenuation of higher frequencies. Tube wave amplitudes constructed from the data obtained with the higher frequency transducer in the 8 centimeter borehole provided the most unambiguous indication of open fractures. The superior quality of these amplitude logs was attributed to the strong excitation of tube waves, as opposed to the primary excitation of the first normal mode by the two lower frequency transducers in the 17 centimeter borehole.

INTRODUCTION

The in situ characterization of the engineering and hydraulic properties of fractured crystalline rocks is one of the most difficult problems in the design of a proposed radioactive waste storage facility. Previous studies have shown the tremendous uncertainty involved in extrapolating laboratory tests performed on small core samples to the behavior of large rock bodies under the level of thermal stress that would be imposed by the storage of high level waste (Goodman,1976). Acoustic waveforms obtained from downhole logging systems

have therefore become an important research tool in the characterization of fractures deep within large bodies of rock (Aki et al, 1982). This renewed interest in the analysis of borehole waveforms has resulted in the discovery that the seismic radiation pattern associated with conventional acoustic logging systems is a great deal more complicated than previously supposed. The details of this radiation pattern depend upon the dimensions of the acoustic logging tool, the diameter of the borehole, and the frequency content of the source transducer, as well as the seismic velocities and densities of the borehole fluid and surrounding rock. This theory has been outlined in recent papers by Cheng and Toksöz (1981), Paillet and White (1982) and Paillet (1981, 1983). It is now generally accepted that the dependence of waveform character on acoustic energy input is a much more complicated function than the simple ratio of acoustic wavelength to borehole diameter used by Biot (1952). The study described here was undertaken as a verification of the theory presented by the authors cited above, and as a test of the ways in which this theory can be used to predict the effectiveness of various velocity picking and attenuation measurement schemes.

The theory presented in the series of papers by Biot (1952), Cheng and Toksöz (1981), and Paillet and White (1982) was formulated for a cylindrical logging tool centralized in a fluid-filled borehole, and surrounded by a homogeneous formation characterized by uniform seismic velocities (V_c, compressional velocity, and V_s, shear velocity), and a constant density. The study site was chosen on the basis of previous results showing that the available boreholes penetrated homogeneous rocks closely approximating the conditions assumed in the theory. In addition to a generalized verification of the theory, this investigation was planned with several practical applications of acoustic waveform logging in mind. For example, shear velocity data can be combined with more readily derived values for compressional velocity and bulk density to specify the effective elastic properties of a rock body (White, 1965). This study will examine the effects of the different transducer frequencies and different borehole diameters on the results from several different shear velocity picking routines in the anticipation that the available theory can be used to understand how such routines work, and to suggest ways in which their performance might be improved.

A second application of great importance in waste disposal research is the characterization of fractures. Previous studies have indicated that tube wave and shear head wave amplitudes can be related to fracture properties (Paillet, 1980; Paillet and White, 1982), but almost all applications to fracture characterization have involved a single acoustic energy source. Length and time scales associated with oscillatory flow within fracture openings may make certain frequencies especially effective in fracture characterization. For example, there may be a characteristic frequency associated with attenuation of oscillations in fluid-filled fractures that is analogous to the characteristic frequency (f_c) derived by Biot (1956) for a porous sandstone model:

$$f_c = \left[\frac{\eta \varphi}{K \rho_f} \right]$$

where φ and K denote the porosity and permeability of the sandstone model, and η and ρ_f denote the viscosity and bulk density of the fluid filling the pore spaces. This investigation therefore considers the effects of variable acoustic source frequencies on amplitude logs and other processed waveform data

displays as used by various fracture characterization approaches (Paillet, 1980; Christiansen, 1964; Pickett, 1963).

STUDY SITE AND EQUIPMENT

The study site is located approximately 10 kilometers (km) east of the town of Lac Dubonnet in southeastern Manitoba, Canada. The three boreholes logged at the site were drilled as part of a research effort sponsored by the Atomic Energy of Canada Limited under the supervision of the Geoscience Branch, Whiteshell Nuclear Research Establishment. One well was completely cored to a diameter of approximately 8 centimeters (cm). The other two wells were drilled to a diameter of approximately 17 cm with periodic analysis of cutting samples. The two 17 cm diameter wells were located within approximately 100 meters (m) of the cored well. The three boreholes penetrate to depths of more than 350 m in the granitic rocks of a batholith located along the southwestern margin of the Superior Province of the Canadian Shield. The homogeneity of the granitic rock comprising this batholith has been demonstrated by Paillet (1980), where various estimates of shear and compressional velocities were shown to closely approximate the velocities from a single fully-saturated core sample of Westerly Granite subjected to various effective stresses (Nur and Simmons, 1969). Seismic velocities determined from waveform data obtained near a depth of 350 m also agreed with core measurements made by Annor and Geller (1978) on a series of samples under laboratory stress conditions equivalent to lithostatic pressure at that depth. The seismic velocities determined from the analysis of unfractured intervals in the corehole were identical to those given by Paillet (1980). The rocks in the vicinity of the study site may therefore be assigned a uniform set of seismic velocities over the depth interval of interest (100 to 400 m):

$$V_c = 5.80 \pm .10 \frac{\text{km}}{\text{s}} \quad \text{and} \quad V_s = 3.35 \pm .10 \frac{\text{km}}{\text{s}}$$

These values have been used in the prediction of arrival times and mode excitation functions in the following sections of this report.

The acoustic frequencies used in this study were obtained by attaching three different magnetostrictive source transducers to the same receiver section as indicated in Figure 1. The use of the same receiver section and uphole electronics for the tests insured that all experimental variables except source character remained the same. Source frequencies were varied by using the same magnetostrictive transducer design, with larger cores of magnetostrictive material assumed to provide lower centerband frequencies (White, 1965). Nominal source frequencies were scaled from the diameter and known frequency of the smallest diameter transducer under the assumption that the resonant frequency of the transducer core scaled according to the inverse of transducer core diameter. These values listed in table 1, along with the dominant frequency content of waveforms excited by each of the transducers in the 17 cm diameter borehole.

TABLE 1—Transducer frequencies and approximate source/receiver offsets in seismic wavelengths based on V_s.

Nominal Transducer Frequency (kilohertz)	Effective Transducer Frequency (kilohertz)	Receiver Offset in Wavelengths		
		Near	Mid	Far
34	34	3	5	9
20	14-22	1.5	2.5	4.5
15	12-17	1.5	2.5	4.5

The logging tool illustrated in Figure 1 contained three receiver crystals, only two of which could be selected for digital recording on any given run. The receivers selected for use in this study were chosen to provide data at a comparable number of seismic wavelengths of source/receiver offset in terms of the dominant source frequencies listed in table 1, and based on the rock compressional velocity, V_c. In most cases data were obtained with receivers selected to represent waveforms recorded at three and five wavelengths of source/receiver separation. Digital waveform recordings were made with a 2 microsecond (μs) sampling interval at approximately 15 cm depth intervals. Borehole diameter effects were included in the study by logging the 8 cm diameter corehole with the high frequency transducer. The larger diameters of the two lower frequency transducers prevented their use in the corehole.

RELATION OF WAVEFORM CHARACTER TO TRANSDUCER FREQUENCY

Representative waveforms for the high frequency transducer in the 8 cm diameter borehole, and for all three transducers in the 17 cm diameter borehole are illustrated in Figures 2a and 2b for the 3 and 5 wavelength receivers. The difference in borehole diameter is associated with a large change in overall waveform appearance for the high frequency transducer, while the waveforms obtained with the two lower frequency transducers appear roughly similar in frequency content. Figures 2a and 2b also indicate the predicted arrival times for direct fluid waves from transducer to receiver (T_f), and for critically reflected compressional (T_c) and shear waves (T_s) corrected for the differences in transducer diameter. The shear arrivals can be recognized in all four cases and at both receiver stations, but appear more variable from one recording to the next for the high-frequency/large-borehole-borehole-diameter case than for the other three cases even for sections of the boreholes with no indication of fracturing or other anomalous conditions. This is illustrated in Figure 3 where different frequency waveforms from the same depth interval in one of the large diameter boreholes are compared. This interval corresponds to a depth where cuttings and televiewer logs indicate the occurrence of large pegmatite crystals in the borehole wall. Figure 3 illustrates the pronounced effect of this condition on the high frequency waveforms. Similar results over many sections of the larger diameter boreholes indicate that the high-frequency/large-borehole-diameter data are much more sensitive to minor departures from centralization and minor amounts of wall rugosity than the lower frequency data.

Power spectra constructed by the Fast Fourier Transform (FFT) of the waveforms illustrated in Figure 2a are shown in figure 4. The peaks in these power spectra can be compared to the theoretical excitation functions for the tube wave and normal modes in the 8 and 17 cm diameter boreholes illustrated in Figure 5. The predicted mode energies indicate that the high-frequency/large-borehole-diameter data have transducer output centered on frequencies just above cut-off for the third normal mode. There are also secondary peaks in the spectrum near 17 and 28 kHz representing low energy excitation of the two lower modes, which has probably been accentuated by differential attenuation. Differential attenuation refers to the tendency for seismic attenuation to be constant over a given number of wavelengths, a property known as the "constant" Q approximation (White, 1965). Seismic waves traveling through rocks that satisfy this approximation will exhibit spectra with decreasing frequencies because the higher frequencies in the original signal undergo greater attenuation in traveling a fixed distance. Even though the two lower frequency transducers are characterized by distinctly different centerband frequencies, they both apparently excited nearly the same combination of first normal mode and tube wave energy. This becomes especially apparent in Figure 2b at the far receiver station where initial energy input into the second normal mode by the mid-frequency transducer has been reduced by the enhanced attenuation of higher frequencies.

The examples given in Figures 2a and 2b illustrate the way in which borehole diameter influences waveform character through the excitation of shear normal modes. The theory presented by Paillet (1981, 1983) and Paillet and White (1982) indicates that the shear normal modes determine the character of shear head wave arrivals. The excitation functions in Figure 5 therefore determine the character of the observed waveforms over the entire interval starting at the predicted arrival time for the critically-refracted shear wave. For this reason, normal mode content in the composite waveform should also have an important effect on the character of shear arrivals. The effect of mode content on shear arrival character can be illustrated by attempting to scale waveform plots on the basis of frequency and wavelength alone. For example, the low frequency waveforms in the 17 cm borehole are characterized by a frequency of approximately one half that exhibited by the high-frequency/large-borehole-diameter data. If waveform character depends only on the length and time scales imposed by wavelength and frequency, the high frequency waveforms should be made to resemble the low frequency waveforms by plotting both at the same number of wavelengths source/receiver separation, with time scale for the high frequency data stretched by a factor of two. This has been done in Figure 6, with the zero point on the time scale adjusted to account for the larger diameter of the low-frequency transducer. The rescaled waveforms remain clearly different in overall character, so that the difference in mode content has introduced a fundamental difference in character that cannot be removed by simple frequency scaling.

The dynamic range of the waveform digitization system did not permit adequate representation of compressional arrivals at gain settings below saturation for normal mode and tube wave portions of the record. However, the operation of the logging system in the conventional compressional transit time mode was checked by transit time logging of the test sections to verify that all three transducers gave results consistent with the known compressional velocity of 5.85 km/s for both borehole diameter cases. The arrival detection

algorithm built into the system worked effectively in all four cases to within the manufacturer's stated limit of resolution (3 μs/m). The only practical problem encountered was related to the character of the first arrivals for the low-frequency data. Although Figure 2a provides poor resolution of the first arrivals, detailed examination at higher resolution indicated that a recurrent tendency to cycle skip was related to a gradual increase in amplitude from first arrival through shear arrival. More consistent transit time logs could be obtained in some unfractured intervals by picking on a second or third amplitude peak rather than the first arrival in both waveforms.

EFFECT OF FREQUENCY ON SHEAR VELOCITY DETERMINATION

Most recent shear velocity picking methods applied to digitized waveform data are based on the cross-correlation technique described by Scott and Sena (1974). The semblance cross-correlation technique described by Cheng et al (1982) was selected as representative of the best available shear picking methods for application to the four data sets used in this study. Results of the application of this method to the waveforms obtained in a typical unfractured interval in the 17 cm borehole are illustrated in Figure 7. The results with the high-frequency/small-borehole-diameter data were identical to those from the two lower frequency cases in the 17 cm diameter borehole, and are not shown in the Figure. Under the assumption that the range of shear velocities is given by the 3.35 ± 0.10 km/s Figure introduced above, the high-frequency transducer in the 8 cm borehole and the two lower frequency transducers in the 17 cm borehole provide accurate shear velocity information. The high-frequency/large-borehole-diameter case, however, consistently provided shear picks that were 10% too low using the semblance cross-correlation method.

TABLE 2–Shear velocity estimates based on picks indicated in Figure 8.

Near Receiver Pick	Far Receiver Pick	Equivalent Shear Velocity in km/s
a. Low Frequency Transducer		
A	A	6.10
B	B	3.39
C	C	3.35
D	D	3.35
E	E	3.31
F	F	3.31
b. High Frequency Transducer		
A	A	5.26
B	B	5.08
C	C	2.88
D	D	4.23
E	E	2.63
F	F	2.93

Considerable insight into the failure of the cross-correlation technique applied to the high-frequency/large-borehole-diameter data can be obtained by attempting to pick shear velocities by more direct methods. Figure 8 illustrates a series of velocity picks determined by selecting the various peaks, troughs, and zero crossings indicated on the plots. The corresponding velocities obtained with each of these peaks is indicated in table 2. The low-frequency case exhibits a prolonged shear onset with a very regular periodicity that is probably imposed by the first normal mode. The values in table 2 indicate that any pair of initial peaks or troughs in the shear signal can be used to generate shear transit times that agree to within one or two digital time steps with the known 3.35 km/s shear velocity. The exact shear arrival appears somewhat better defined for the high-frequency case in Figure 8 due to the shorter period of the source signal. Attempts to calculate shear arrivals on the basis of peak or trough moveout in this data set produces a wide scatter of results both above and below the true value. Inspection of the waveforms indicates that this results from the large change in shape of shear arrival between receivers. This is probably related to the complicated interference pattern generated by the superposition of three normal modes, and to the change in overall signal produced by the greater attenuation of higher frequencies.

The comparison of waveforms in Figure 8 indicates that the failure of the shear picking algorithm in the high-frequency/large-borehole-diameter case is related to the number of normal modes excited by the transducer. The reduction in amplitude of the second and third normal modes produced by the greater attenuation of higher frequencies apparently leads to the overestimation of shear transit times by the semblance cross-correlation program. At the same time, the relatively poor definition of the shear arrival provided by the oscillatory signal of the combined shear head wave and first normal mode does not prove to be a practical obstacle to accurate estimation of shear transit times. The major difficulty in picking shear arrivals from such data would be the recognition of cycle skips.

FRACTURE CHARACTERIZATION

A second important application of acoustic waveform data is the in situ identification and characterization of fractures in crystalline rock. Various authors have described applications of acoustic waveform data to fracture identification using either the display of waveform traces in a format similar to those used in surface seismic data display (Morris et al, 1965), or the computation of various filtered amplitude logs (Paillet, 1980; Paillet and White, 1982). Acoustic log data has also been used to characterize the bulk properties of fractured rock bodies (Stierman, 1979; Moos and Zoback, 1983). The construction of amplitude logs for several test cases according to the methods described by Paillet (1980) indicated that the combination of high frequency and small borehole diameter was especially favorable for amplitude measurements. Part of the reason for this favorable result may be attributed to the mode content of the data, because the small borehole diameter caused optimal excitation of the tube wave mode. The data appeared very sensitive to the location of either transducer or receiver adjacent to the fracture opening, and this effect could not be related to mode content in any simple way. It was also suspected that the relatively high transducer frequencies were especially

sensitive to low fracture permeabilities by extrapolating the theoretical results given by Rosenbaum (1974) to formations with fracture permeability and no filtercake. Since this effect does not appear to be related to normal mode content either, and since fracture permeability and orientation might provide time scales of their own, the data obtained in this study were used to compare the effects of various transducer frequencies on the ability of waveform displays and amplitude logs to characterize fractured rocks. Previous experience with the granitic rocks at the study site showed that fractures intersecting the boreholes could be classified into several types: 1) isolated horizontal fractures; 2) closely spaced horizontal fractures capable of exciting multiples in the data; 3) steeply dipping fractures that intersect the borehole over a broad depth interval; 4) multiply-intersecting fractures in relatively unweathered rock; and 5) intensely weathered and fractured intervals such as those identified as major shear zones by Mair and Green (1981). The three boreholes used for this study intersected at least two of each of these fracture types.

Most waveform data obtained for this study were recorded with gain settings selected to prevent saturation of the high amplitude portion of the record. As a result, the low-amplitude compressional arrivals were recorded with very low resolution. Several short test sections were therefore run at much higher gain and at a decreased sampling interval of 0.5 μs, providing higher resolution of the low amplitude first arrivals. Analysis of these records indicated that the compressional head wave amplitudes were relatively insensitive to fracture permeability. There were no unambiguous indications of signal reinforcement due to the presence of multiples when horizontal fractures were spaced approximately one wavelength apart. It was simultaneously observed that the primary effect of fracture permeability on the tube waves and later portion of the first normal mode was simple attenuation. The portion of the waveform between shear arrival and direct fluid travel time, however, appeared sensitive to even relatively tight, partially closed fractures. For this reason, displays such as that illustrated in Figure 9 were optimized by emphasizing the portions of the waveform starting at shear arrival. Figure 9 illustrates the waveforms produced by the three transducers in a sample interval containing isolated horizontal and subhorizontal fractures, some of which appear to be open on the televiewer log. These waveforms may be compared to an equivalent display of waveforms in the vicinity of a similar set of isolated horizontal fractures located in the small diameter corehole (Figure 10). The waveforms in Figures 9 and 10 have been plotted for receivers located approximately three wavelengths uphole from the transducer. This offset was selected as the optimum compromise between mode separation and depth resolution. In theory the depth resolution could be improved by taking the difference between amplitudes at two closely-spaced receivers located far enough from the source to allow good mode separation. This approach was not taken, however, because there were many indications that the primary contribution to waveform anomalies in the vicinity of permeable fractures was related to interaction between the source transducer and the fracture opening. In that case, the differencing of receivers would reject the most significant source of information about fracture character as discussed by Paillet (1980).

The waveform log and the depth-correlated televiewer log Figure 9 indicate that the fractures shown on the televiewer log produced recognizable anomalies in waveform propagation at all three frequencies. The response of

the two lower frequencies is roughly similar, as would be expected from the similarity in frequency content. The two lower frequency transducers also appear to produce a more regular response than the high-frequency transducers, but none of the data sets from the large diameter boreholes appears to bear as simple an interpretation as the corresponding data sets for the high frequency transducer in the 8 cm borehole.

Tube wave and normal mode amplitude logs were constructed for the waveforms illustrated in Figure 9 and 10 by convolving the mean square amplitude in windows starting at direct fluid arrival time with a half-cosine filter. These amplitude logs have been aligned with the corresponding section of the televiewer log in Figure 11. The amplitude logs indicate that none of the three transducers in the 17 cm borehole respond to isolated fractures with the simple, consistent deflections in amplitudes observed for the high frequency transducer in the 8 cm diameter borehole. Although Figures 9-11 offer a limited sample of the fracture anomalies observed in the waveform data set, they have been selected as representative examples of the results obtained from several such zones of isolated fractures. The most probable reason behind the difference between the amplitude logs for the large and small diameter borehole waveforms is the difference in mode content: even the lowest frequency data for the larger borehole are dominated by the first normal mode, while the primary contribution to the late amplitudes in Figure 10 comes from the tube wave alone.

An additional reason for considering the use of lower frequency transducers in the larger diameter boreholes was the hope that the slightly longer wavelengths would provide more effective penetration in more heavily fractured and weathered zones. An example of waveforms obtained with all three frequency transducers in the vicinity of one such heavily fractured interval is given in Figure 12. The lower frequency transducers have produced anomaly patterns that appear slightly more regular, but the corresponding amplitude logs show no dramatic improvement when the frequency is lowered by using the two lower frequency transducers. Perhaps such an improvement would have been realized if the lowest frequency transducer had excited a dominant tube wave response rather than the observed mixture of tube wave and lowest normal mode.

CONCLUSIONS

A controlled experimental study of acoustic waveform propagation in boreholes penetrating a homogeneous granitic formation has demonstrated that waveforms do scale with borehole diameter and source frequency according to theory. Recorded borehole waveforms are characterized by frequency components imposed by borehole geometry and seismic velocities through the excitation of a specific set of modes, and not by the centerband frequency of the acoustic source alone. In cases where more than one normal mode is excited, the differential attenuation of higher frequencies may cause a significant change in periodicity between receivers. This effect is an important factor in the effectiveness of shear picking programs. The superposition of multiple normal modes leads to large changes in phasing of the shear arrivals between stations, often introducing significant error into the shear velocity

picking process. At the same time, waveforms dominated by a single normal mode have shear arrivals characterized by a highly oscillatory signal with an easily-recognized phase velocity. Previous authors have suggested that the dispersive nature of the normal modes might introduce errors in shear velocity measurement, but this appears to less of a practical problem here than the effects of multiple normal modes. This phenomenon may also explain the popularity of the ultra-long-spaced waveform logging systems (Koeperich, 1979; Arditty et al, 1982), because the long source/receiver offsets allow attenuation of all the higher normal modes, and therefore remove the interference effects described here.

An important objective of this study was the search for a method equivalent to the tube wave method described by Paillet (1980) and Paillet and White (1982) that could be applied to larger diameter boreholes without encountering the operational problem of stuffing a logging tool into a very small diameter borehole. The logical approach was to reduce the frequency of the acoustic energy source in compensation for the larger annulus between tool and borehole according to the scaling described by Cheng and Toksöz (1981). The lower frequencies used here did appear to give some improvement in fracture characterization, but did not produce simple amplitude anomalies equivalent to those obtained with the higher frequency source in the 8 cm diameter borehole. This result may stem from the fact that the lowest frequency transducer did not produce waveforms dominated by the tube wave, although a tube wave contribution to the composite waveform was apparently present. It is still unclear whether the good results illustrated in Figure 10 and described in detail by Paillet (1980) stem directly from the nature of the tube wave itself, or from a fortuitous tuning of source frequencies to fracture properties that results in especially effective tube wave logs. Except for this important qualification, this study indicates that optimal display of full waveform acoustic data should include scaling to emphasize shear and normal mode arrivals, and logging equipment with transducer frequencies or source/receiver spacings designed to produce waveforms dominated by tube waves or a combination of tube waves and the first normal mode.

ACKNOWLEDGEMENTS

The author appreciates the cooperation of Cliff Davison and others from the Whiteshell Nuclear Research Establishment, Atomic Energy of Canada Limited in obtaining access to the test wells at the URL. W. Scott Keys, Richard Hodges and Alfred Hess provided valuable assistance in running the televiewer logs used in this study. The Earth Resources Laboratory, Massachusetts Institute of Technology, provided computational facilities and other support for the work performed in the preparation of this report.

REFERENCES

Aki, K., Fehler, M., Aamodt, R. L., Albright, J. N., Potter, R. M., Pearson, C. M., and Tester, J. W., 1982, Interpretation of seismic data from hydraulic fracturing experiments at Fenton Hill, New Mexico, hot dry rock geothermal site, Journal of Geophysical Research, v. 87, p. 936-944.

Annor, A. and Geller, L., 1978, Dilitation velocity, Young's modulus, poisson ratio, uniaxial compression test and resilient compression test tensile strength for WN1 and WN2 samples: CANMET Mining Research Laboratory Technical Data, 303410-M01/78.

Arditty, P. C., G. Arens, and Ph. Staron, 1982, State of the art on EVA processing: an improvement in subsurface imaging, Technical Program Abstracts, 52nd Annual International Meeting of the Society of Exploration Geophysicists, Dallas, Texas, p. 322-325.

Biot, M. A., 1952, Propagation of elastic waves in a cylindrical bore containing a fluid, Journal of Applied Physics, v. 23, p. 997-1009.

Biot, M. A., 1956, Theory of propagation of elastic waves in a fluid-saturated porous solid, I low frequency range, Journal of the Acoustical Society of America, v. 28, p. 168-178.

Cheng, C. H. and Toksöz, M. N., 1981, Elastic wave propagation in a fluid-filled borehole and synthetic acoustic logs, Geophysics, v. 46, p. 1042-1053.

Cheng, C. H., Toksöz, M. N., and Willis, M. E., 1982, Determination of in situ attenuation from full waveform acoustic logs: Journal of Geophysical Research, v. 87, p. 5477-5484.

Christiansen, D. M., 1964, A theoretical analysis of wave propagation in fluid-filled drill holes for the interpretation of three dimensional velocity logs, 5th Annual Logging Symposium of the Society of Professional Well Log Analysts, Midland, Texas, p K1-K31.

Goodman, R. E. ,1976, Methods of geological engineering in discontinuous rocks, St. Paul, Minnesota, West Publishing Company, 472 pp.

Koeperich, E. A., 1979, Shear wave velocities determined from long and short spaced acoustic devices, Society of Petroleum Engineers, Institute of Mining and Metallurgy Engineers, Paper SPE 8237, 12 pp.

Mair, J. A., and Green, A. G., 1981, High resolution seismic reflection profiles reveal fractures within a homogeneous granite batholith, Nature, v. 294, p. 439-442.

Moos, Daniel and Zoback, M. D., 1983, In situ studies of velocity in fractured crystalline rocks, Journal of Geophysical Research, in press.

Morris, R.L., Grine, and Arkfield, T. E., 1965, Using compression and shear acoustic amplitudes for the location of fractures, Journal of Petroleum Technology, v. 13, p. 623-632.

Nur, A. M. and Simmons, G., 1969, The effects of saturation on velocity in low porosity rocks, Earth and Planetary Science Letters, v. 7, p. 183-193.

Paillet, F. L., 1980, Acoustic propagation in the vicinity of fractures which intersect a fluid-filled borehole, 21st Annual Logging Symposium of the Society of Professional Well Log Analysts, Lafayette, Louisiana, 33 p.

----------, 1981, Predicting the frequency content of acoustic waves in boreholes, 22nd Annual Logging Symposium of the Society of Professional Well Log Analysts, Mexico City, Mexico, 26 p.

----------, 1983, Comprehensive theory for the interpretation of compressional and shear head waves in boreholes, in press.

Paillet, F. L. and White, J. E. ,1982, Acoustic normal modes in the borehole and their relationship to rock properties: Geophysics, v. 47, p. 1215-1228.

Pickett, G. R., 1963, Acoustic character logs and their application in formation evaluation: Journal of Petroleum Technology, v. 15, p. 659-667.

Rosenbaum, J. H., 1974, Synthetic microseismograms: logging in porous formations: Geophysics, v. 39, p. 14-32.

Scott, J. H., and Sena, J., 1974, Acoustic logging for mining applications: 15th Annual Logging Symposium of the Society of Professional Well Log Analysts, McAllen, Texas, 11 p.

Stierman, D. J., and Kovach, R. L., 1979, An in situ velocity study: the Stone Canyon well: Journal of Geophysical Research, v. 84, p. 672-683.

White, J. E., 1965, Seismic waves: radiation, transmission and attenuation, New York, McGraw-Hill, 380 p.

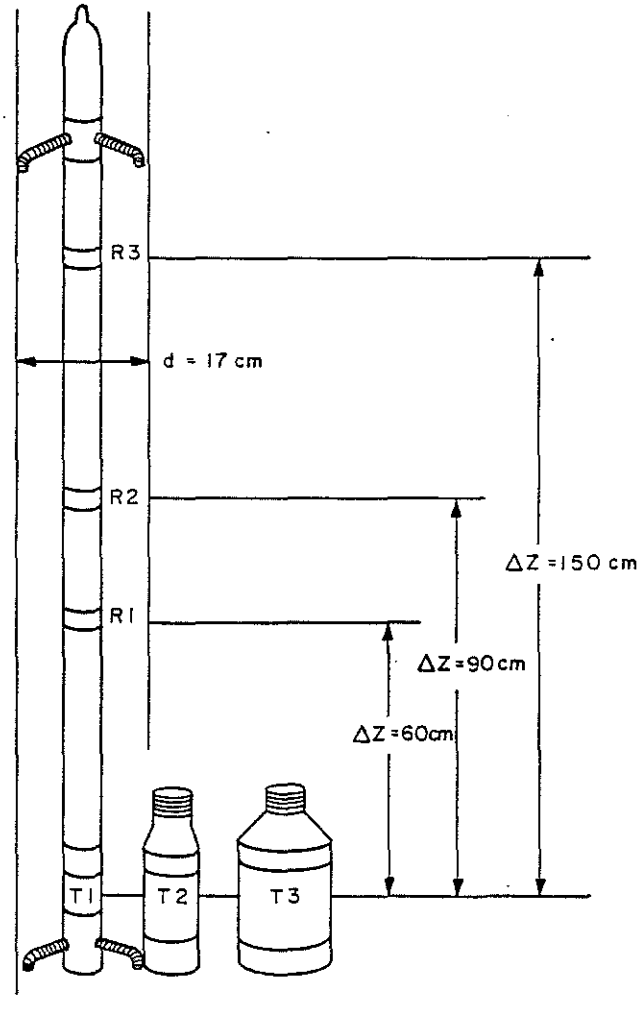

Figure 1. Schematic illustration of logging tool indicating relative size of transducers and source/receiver separations in the 17 cm diameter borehole.

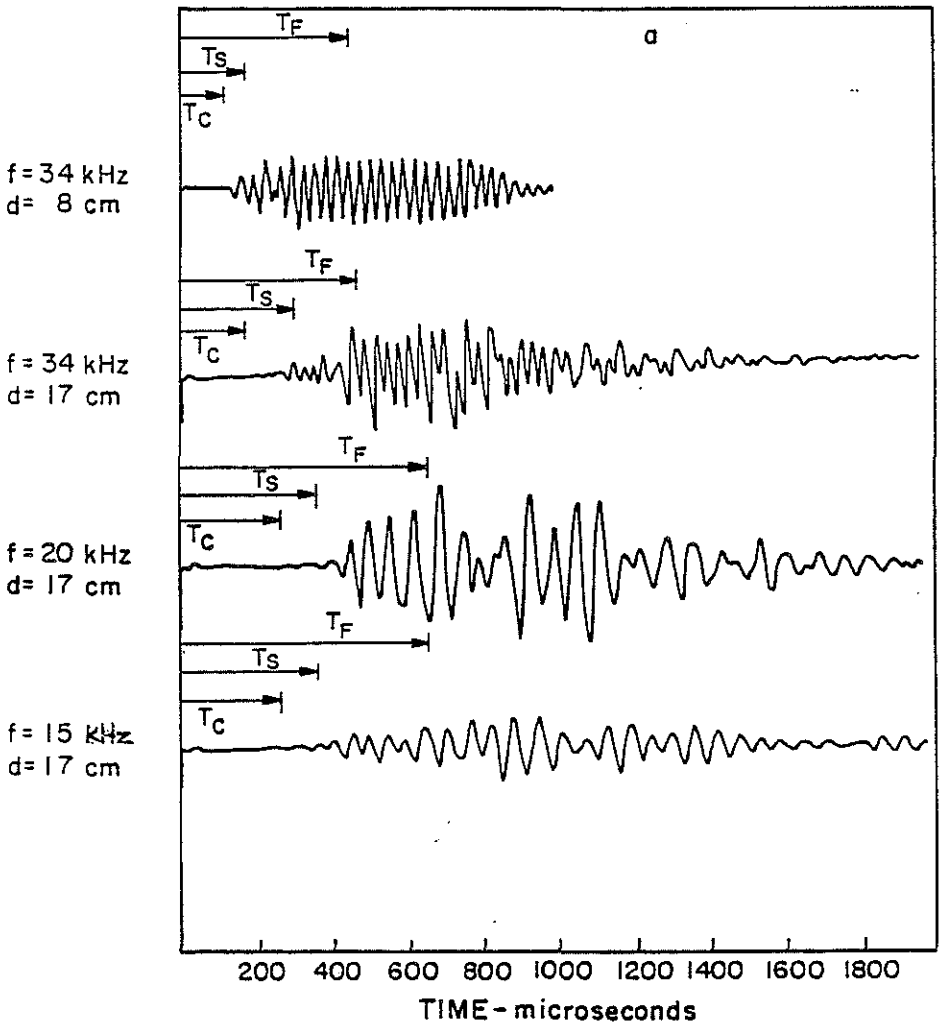

Figure 2a. Sample waveforms in unfractured rocks for the data cases indicated at three seismic wavelengths of source/receiver separation.

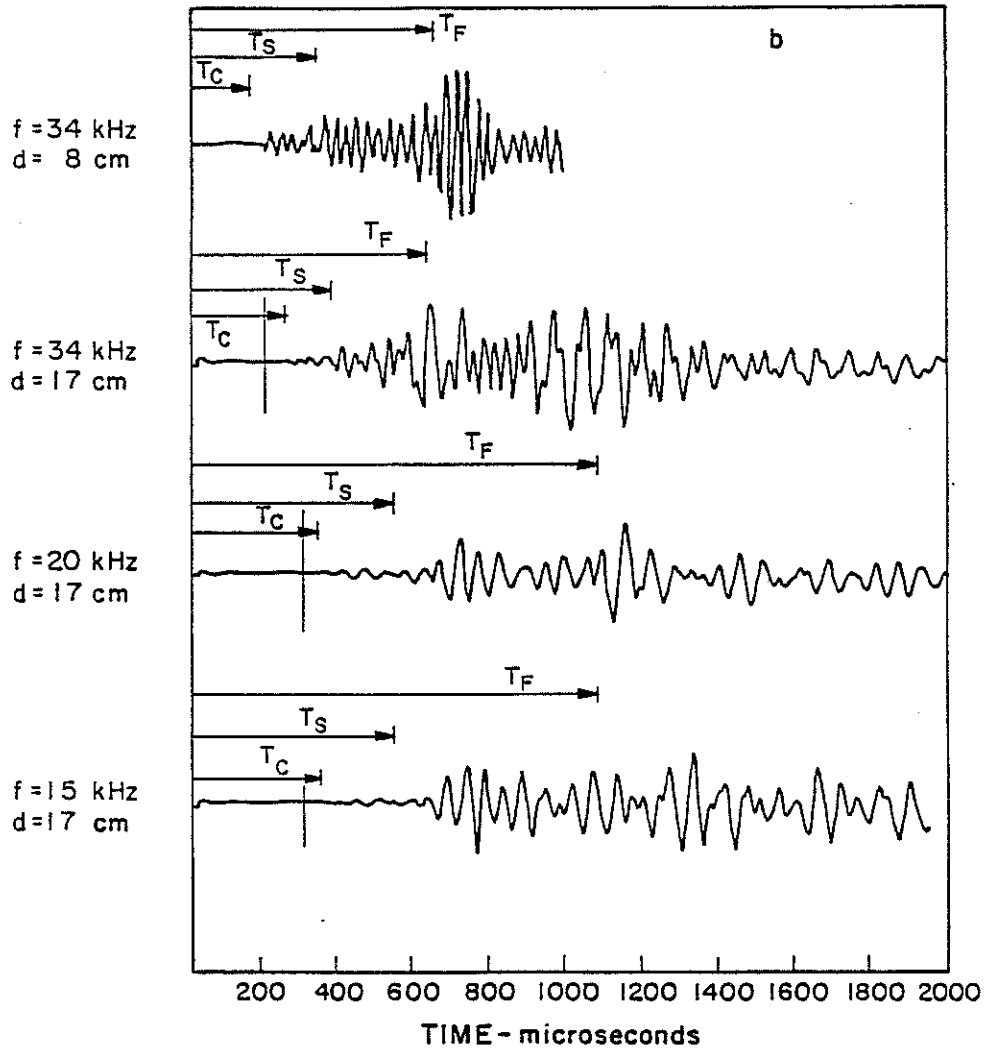

Figure 2b. Sample waveforms in unfractured rocks for the data cases indicated at five seismic wavelengths of source/receiver separation.

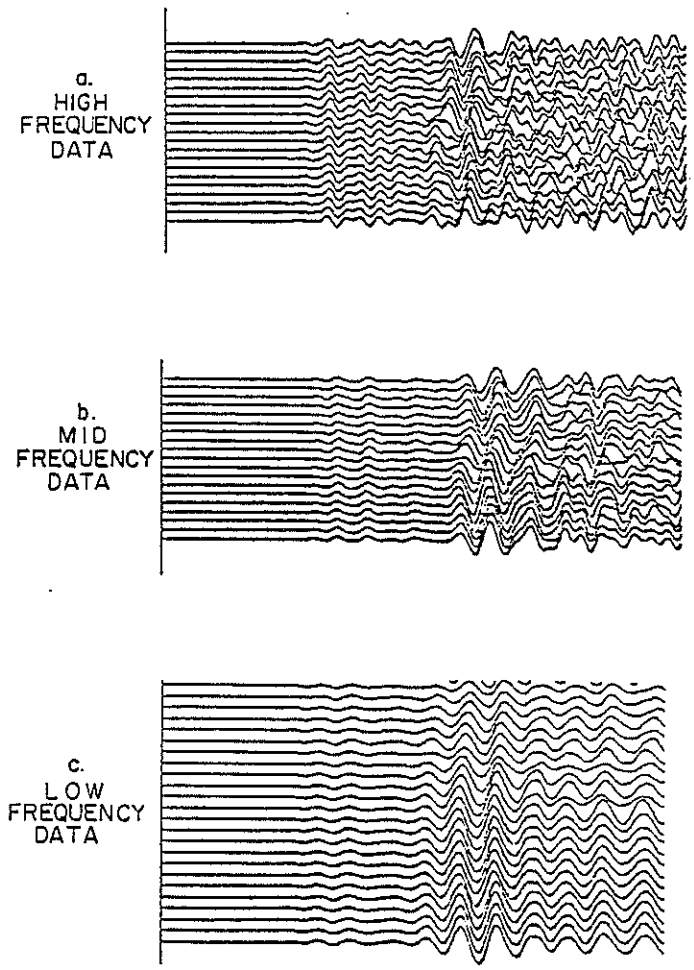

Figure 3. Comparison of waveforms in the 17 cm diameter borehole illustrating data for a) high-frequency transducer, b) mid-frequency transducer, and c) low-frequency transducer.

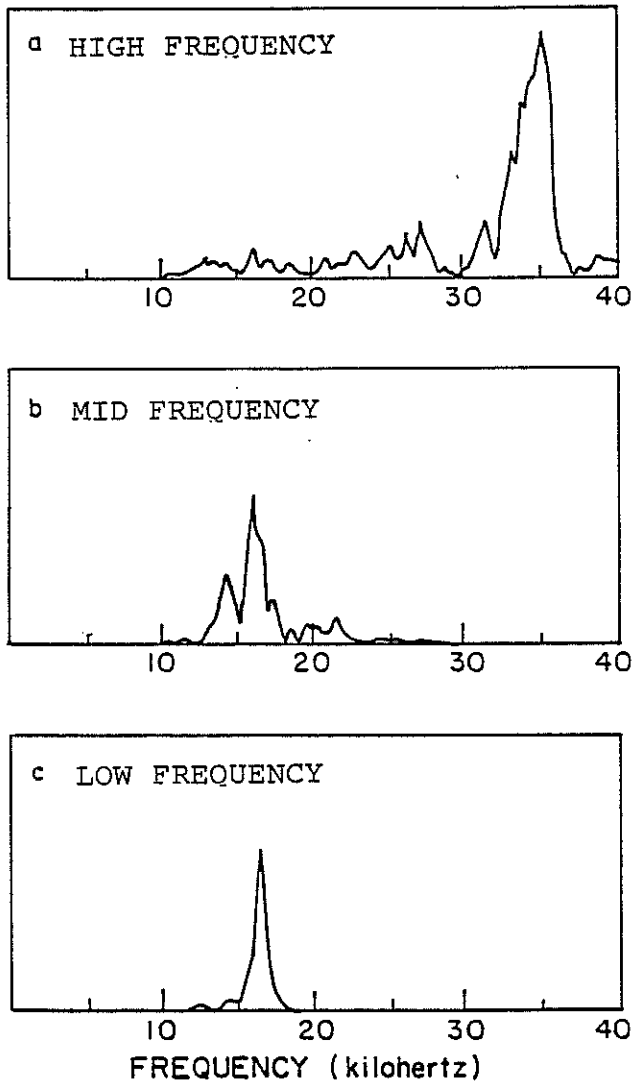

Figure 4. Power spectra for waveforms at 3 seismic wavelength source/receiver separation in large diameter borehole.

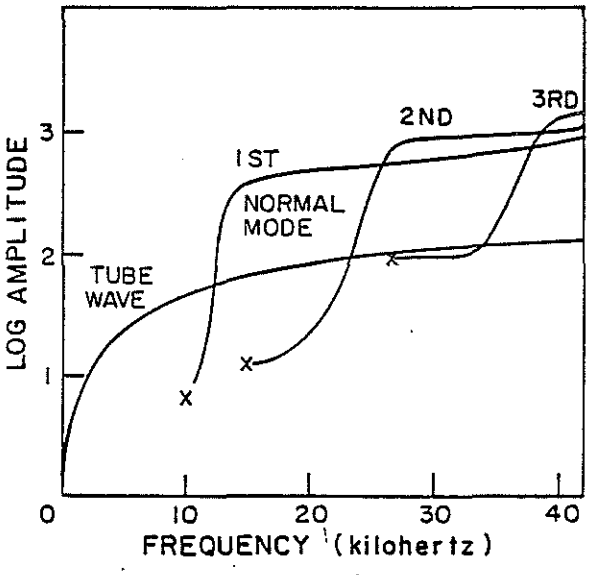

Figure 5. Theoretical excitation functions for 17 cm diameter borehole filled with water and surrounded by homogeneous granite.

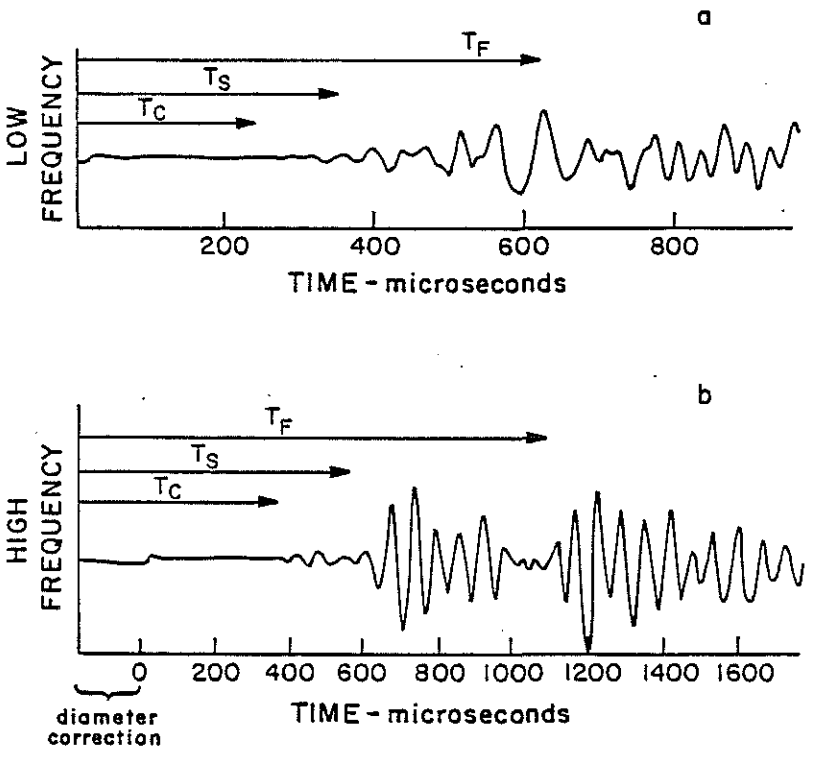

Figure 6. Comparison of a) high-frequency waveforms and b) low-frequency waveforms in the 17 cm diameter borehole with time scales normalized by frequency, and at approximately 3 seismic wavelengths source/receiver separation.

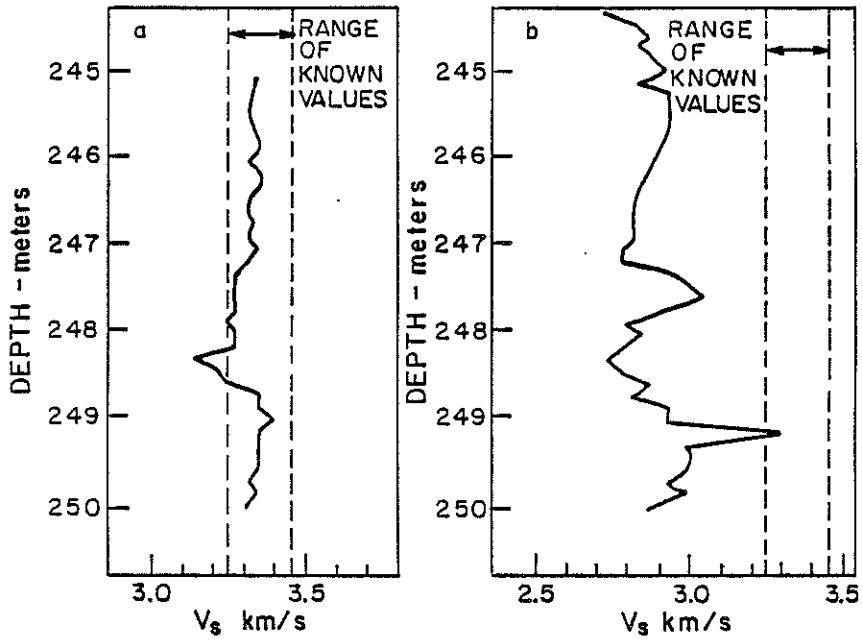

Figure 7. Shear velocities determined by semblance cross-correlation for a) low-frequency data and b) high-frequency data in the 17 cm diameter borehole.

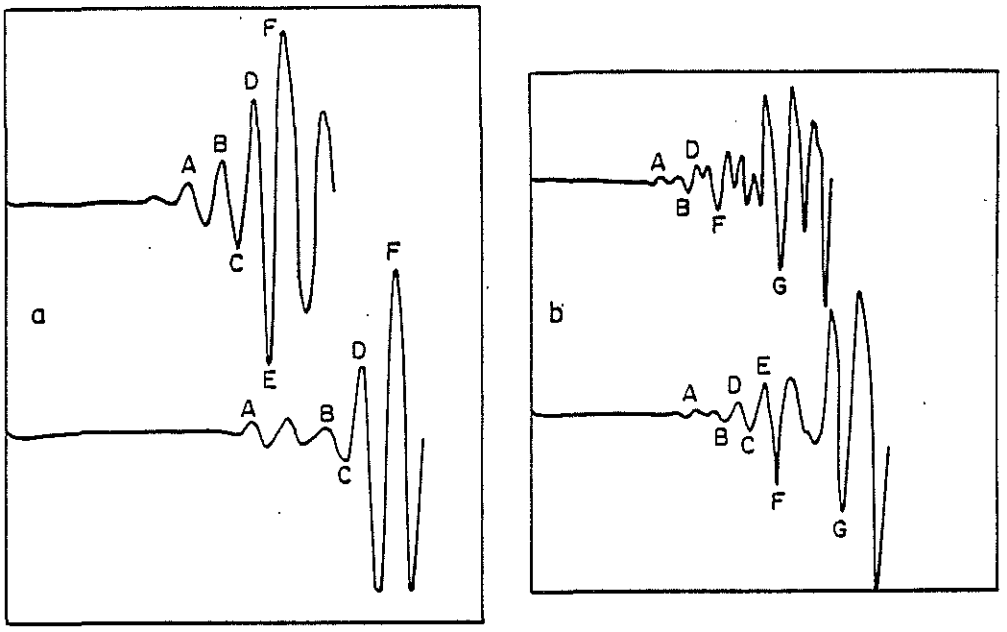

Figure 8. Sample waveforms for a) low-frequency source and b) high-frequency source in large diameter borehole showing various picks for shear arrival.

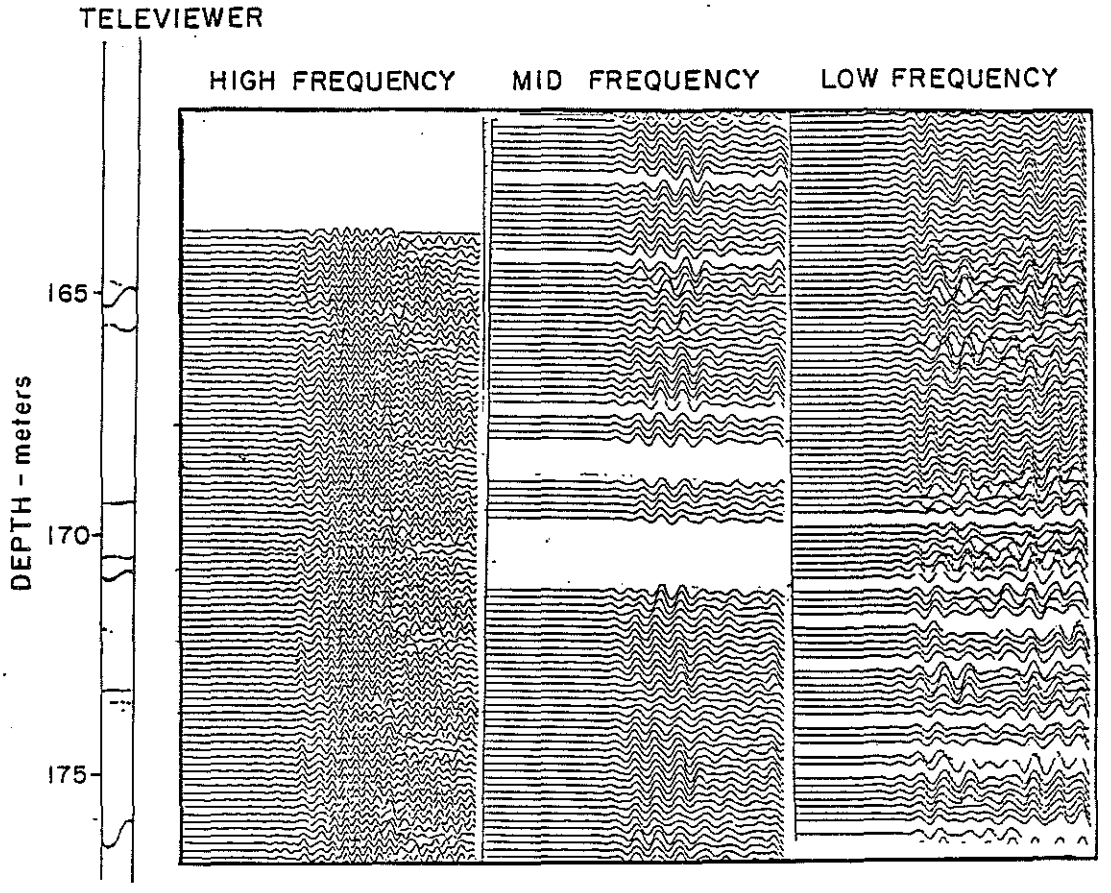

Figure 9. Typical waveform anomalies in data obtained with three different transducers in the large diameter borehole compared to depth-correlated televiewer log.

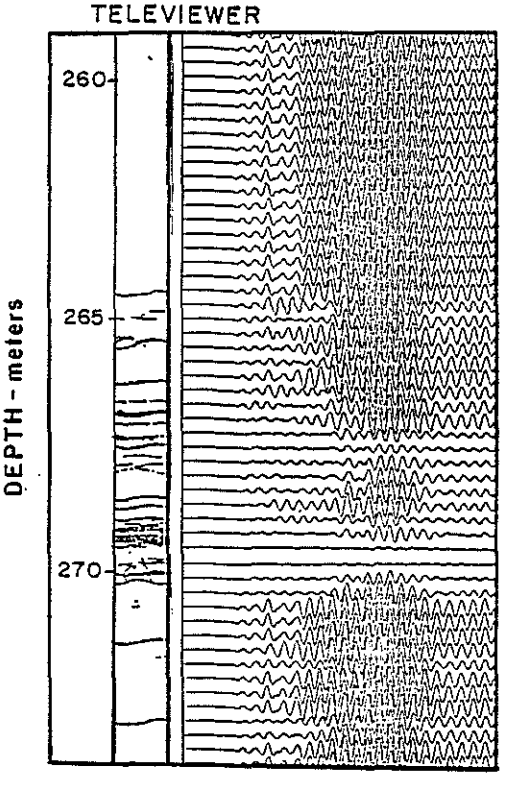

Figure 10. Typical fracture anomalies in waveform data from small diameter borehole; high-frequency transducer only.

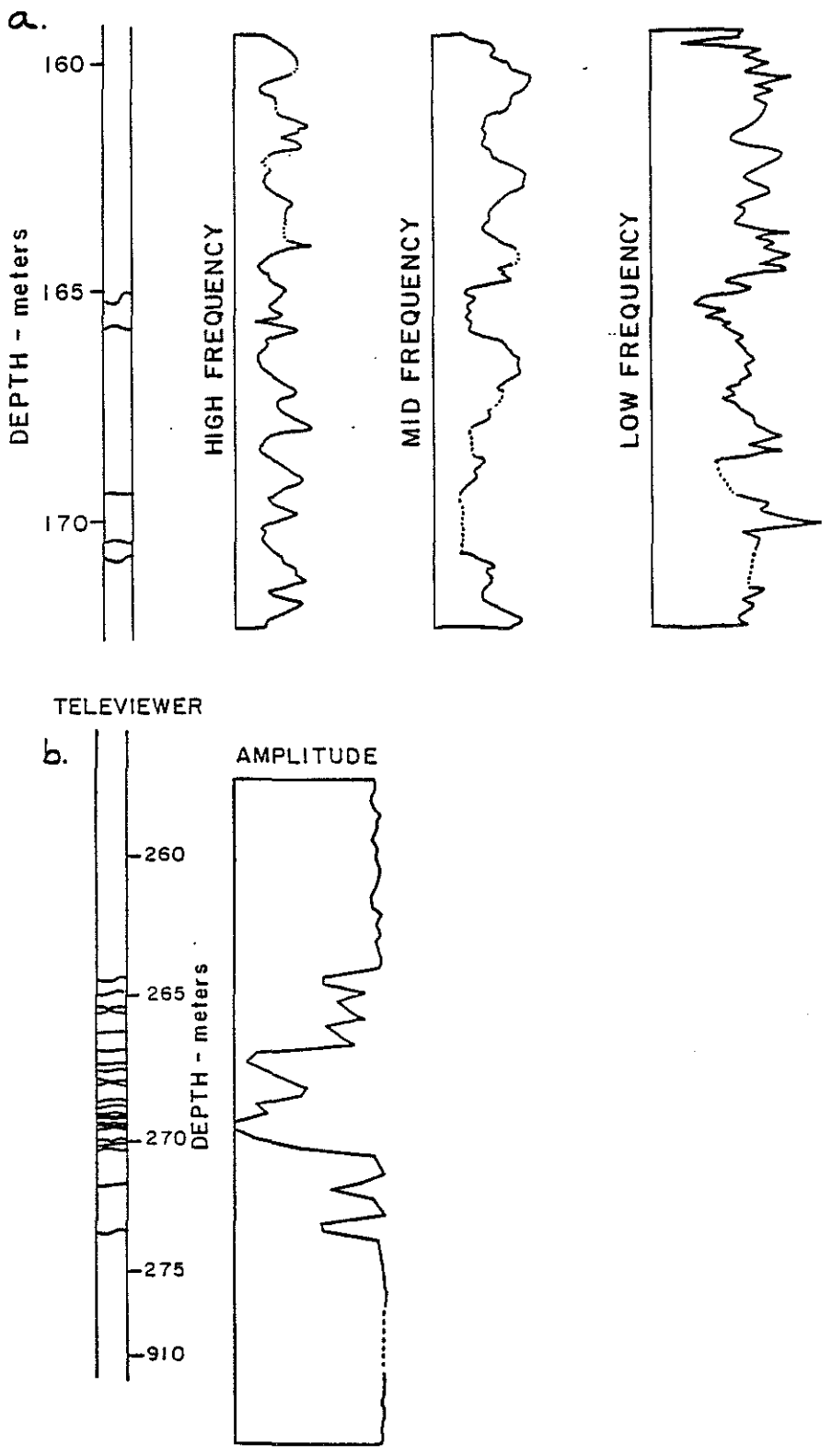

Figure 11. Acoustic amplitude logs constructed from waveform data illustrated in a) Figure 8, and b) figure 9.

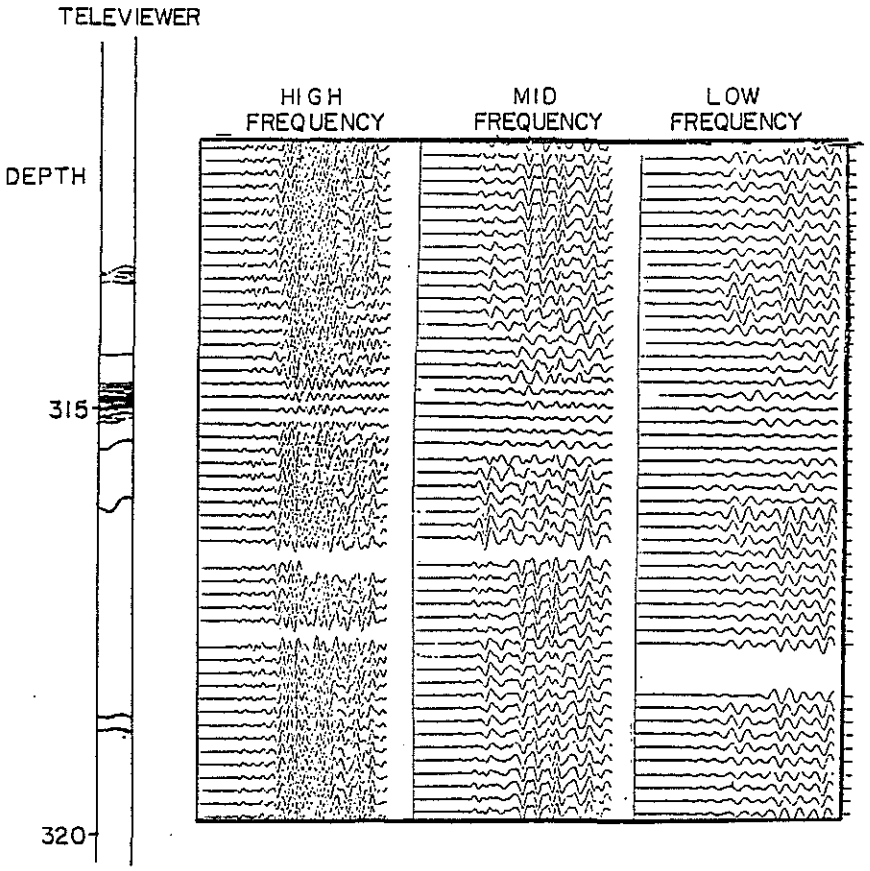

Figure 12. Waveform anomalies in data obtained with all three transducers over a depth interval containing a major fracture zone.